IEEE Access
Multidisciplinary | Rapid Review | Open Access Journal

Received June 4, 2019, accepted July 2, 2019, date of publication August 13, 2019, date of current version October 25, 2019.

Digital Object Identifier 10.1109/ACCESS.2019.2935161

First in Canada, Night and Day Field Demonstration of a New Photovoltaic Solar-Based Flexible AC Transmission System (FACTS) Device PV-STATCOM for Stabilizing Critical Induction Motor

RAJIV K. VARMA[1], (Senior Member, IEEE), EHSAN M. SIAVASHI[1], (Member, IEEE), SIBIN MOHAN[1], (Student Member IEEE), AND TIM VANDERHEIDE[2], (Member, IEEE)

[1]ECE Department, The University of Western Ontario, London, ON N6A 5B9, Canada
[2]Bluewater Power Distribution Corporation, Sarnia, ON N7T 7L6, Canada

Corresponding author: Rajiv K. Varma (rkvarma@uwo.ca)

This work was supported in part by the Ontario Centres of Excellence (OCE), Bluewater Power Distribution Corporation, Sarnia, under Grant CR-SG30-11182-11, in part by the University of Western Ontario WSS-NSERC-Accelerator Grant, and in part by the Natural Sciences and Engineering Research Council of Canada (NSERC).

ABSTRACT Photovoltaic (PV) solar farms are typically dormant at nighttime with their entire expensive assets unused. This paper presents the first in Canada (and perhaps first in the world) utility demonstration of a novel nighttime and daytime technology of utilizing PV solar farm as a dynamic reactive power compensator (STATCOM), and named PV-STATCOM. The field demonstration was performed on a 10 kW PV solar farm installed in the utility network of Bluewater Power Distribution Corporation, in Sarnia, Ontario. It is demonstrated that the solar farm autonomously transforms into a STATCOM and ensures continuous stable operation of a critical induction motor during large disturbances which would otherwise destabilize the motor. The PV-STATCOM is thus shown to be a new FACTS device STATCOM which provides a 24/7 dynamic voltage control functionality as a STATCOM but is about 50 times less costly than an actual equivalent sized STATCOM. The PV-STATCOM is further demonstrated to be a new smart inverter which operates much faster than a conventional smart inverter and also during nighttime, which present-day smart inverters do not. Shutdown of critical induction motors used in industries such as petrochemicals, process control, mining, automotive, medicines, etc. can result in significant financial loss to the industries. This novel functionality of critical motor stabilization by solar farms as PV-STATCOM can potentially open a substantial new revenue earning opportunity for solar farms in addition to generation of active power. This paper presents the first stage results of field demonstration of PV-STATCOM technology on 13th Dec. 2016, in an ongoing project.

INDEX TERMS Flexible AC transmission system (FACTS), photovoltaic (PV) solar systems, STATCOM, distributed generators, distributed energy resource, smart inverter, PV-STATCOM, voltage control, reactive power control, induction motor.

I. INTRODUCTION

Flexible AC Transmission Systems (FACTS) are high power electronic devices which are widely used worldwide for providing several benefits to electric power systems. These include dynamic voltage control, enhancing power transmission capability, improving steady state and transient stability, increasing damping of power oscillations, preventing voltage instability, stabilizing critical motors, mitigating subsynchronous resonance, improving High Voltage DC (HVDC) converter terminal performance, correcting power factor, integrating renewable energy systems such as wind power systems and Photovoltaic (PV) solar power systems, etc. [1]–[3]. Static Var Compensator (SVC) and Static

The associate editor coordinating the review of this article and approving it for publication was Sofana Reka S.

Synchronous Compensator (STATCOM) are two major shunt-connected FACTS devices that provide the above functions through dynamic reactive power compensation. SVC responds within 2-4 cycles while STATCOM provides a faster response within 1-2 cycles, and is consequently more expensive than SVC.

An important application of SVCs and STATCOMs is stabilization of critical induction motors during system disturbances and faults. 80% of all industrial motors are induction motors (IMs), as they are rugged, reliable and economical [4], [5]. IMs are however sensitive to voltage fluctuations, and a large system disturbance can lead to their shutdown especially in weak networks due to inadequate reactive power support [6], [7]. Shutdown of these IMs, even for a short duration of few minutes, can result in significant economic loss to the industrial facilities as the entire batch of materials being transported/served by these motors may get damaged [8], [9]. In one petrochemical industry (name withheld for confidentiality) the loss caused by the shutdown of motors is estimated to be $ 1 Million for just one hour of the shutdown.

Conventionally, STATCOMs or SVCs are installed at the terminal of critical IMs to prevent instability [2], [10]. Dynamic voltage support by SVC prevents stalling of IM during system disturbances [11], [12]. The superiority of STATCOM over SVC in alleviating voltage overshoots during asymmetrical faults and ensuring faster recovery of IM speed was demonstrated in [13]. In a gold mine in Matachewan, Ontario, six 4.5 Mvar STATCOMs are installed to provide dynamic reactive power support for IMs fed by long cables [14]. In a petrochemical plant in Texas, a 16.8 Mvar STATCOM is connected to provide stability to large motors [14]. A 5 Mvar STATCOM is employed to provide dynamic reactive power support to critical motors at Seattle Iron and Metal Corporation [15]. It is however noted that both SVC and STATCOM are very expensive devices.

PV solar systems are growing at an unprecedented rate around the world in the last decade. It is expected that PV systems which had a global installed capacity of 398 GW in 2017 [16] will grow to 8500 GW and provide more than 35% of global electricity in 2050 [17]. To better utilize solar systems, several grid codes and Standards are now requiring PV solar systems to provide various voltage and frequency related grid support functions [18]–[21].

During 2012-16, EPRI developed the concept of ''smart inverter'' (also known as advanced inverters) according to which PV inverters can provide different grid support functions through reactive and real power control, in addition to the generation of real power [22]. These functions include volt-var control, volt-watt control, frequency-watt function, dynamic reactive current, Low/High Voltage Ride Through (L/HVRT), Low/High Frequency Ride Through (L/HFRT), peak power limiting, ramp rate control, etc., [22]. It is noted that voltage control functions such as volt-var and volt-watt have a typical response time of 1-3 seconds [20]–[22].

Prior to 2016, field demonstrations of smart inverter functions for voltage control such as fixed (non-unity) power factor, volt-var and volt-watt, etc. were performed by utilities [23], [24]. The fixed power factor operation of utility scale rooftop PV plants for mitigation of voltage related issues due to PV integration was demonstrated on a 2 MW PV system in California [23]. The effectiveness of fixed power factor smart PV inverter function in reducing voltage deviations was field-demonstrated on a distribution circuit near Porterville, California, for increasing hosting capacity of PV systems [24]. The results of field demonstration of smart inverters with volt-var control and power factor control for providing voltage support in San Diego Gas & Electric (SDG&E) distribution network were presented in [25]. A demonstration project was conducted in Puerto Rico on two utility-scale photovoltaic (PV) plants rated 20+ MW to demonstrate power smoothing, frequency regulation services and power quality [26]. In all the above utility demonstrations, the voltage control based smart inverter functions had a response time of 1-3 seconds and furthermore, these were not demonstrated during nighttime.

In 2009, a new technology of utilizing PV solar farms as STATCOM, was proposed for increasing the connectivity of neighbouring wind farms on distribution systems [27]. This technology was named PV-STATCOM and utilized to increase system stability and enhance power transmission capacity of existing lines [28], [29]. This technology used the entire PV inverter capacity during nighttime and the inverter capacity remaining after real power production during daytime for STATCOM operation. A limitation of this technology was non-availability of any inverter capacity during noontime i.e., periods of full solar power production. In 2014, this technology was enhanced to utilize the entire inverter capacity at any time during system need in the day, as STATCOM [30]. The PV-STATCOM technology thus enables a PV solar farm to provide a 24/7 functionality as a STATCOM. As a precursor to field demonstration, the PV-STATCOM control for night and day was tested on static loads in a lab environment and results were presented in [31].

On 13th December 2016, the PV-STATCOM technology was field-demonstrated in the night and day for the first time in Canada, and perhaps in the world, on a 10 kW PV solar system in the utility network of Bluewater Power Distribution Corporation, Sarnia, Ontario [32]. The solar farm was shown to autonomously transform into a PV-STATCOM during large disturbances both in the night and day and ensure continuous stable operation of a critical induction motor, which would have otherwise become unstable. As mentioned earlier, typically STATCOMs or SVCs are utilized for this purpose. However, PV-STATCOM technology provides the same functionality as an equivalent sized STATCOM or SVC at about 50 times lower cost, as explained later in this paper.

This paper presents detailed results of the first-stage utility-demonstration of PV-STATCOM technology for critical motor stabilization. The key paper contributions are:

(i) it presents the first in Canada (and most likely the first in the world) field-demonstration results of a novel

control of PV solar farm as STATCOM, termed PV-STATCOM.

(ii) it demonstrates the effectiveness of PV-STATCOM control to stabilize a critical induction motor during nighttime when conventional solar farms are idle and also during daytime.

(iii) it shows that the PV-STATCOM provides dynamic reactive power control at the same response speed (1-2 cycles) as a conventional STATCOM.

The 10 kW PV-STATCOM installed in the Bluewater Power Distribution Corporation network is operating satisfactorily since the first demonstration. More new controls have been being added and new applications are being studied, which will be reported in a separate paper.

The rest of this paper is organized as follows. The study system is described in Section II. The PV-STATCOM technology is discussed in Section III. The PV-STATCOM Controller and Operation Mode Selector are presented in Sections IV and V, respectively. The Field demonstration results are described in Sec.VI. The paper is concluded in Section VII.

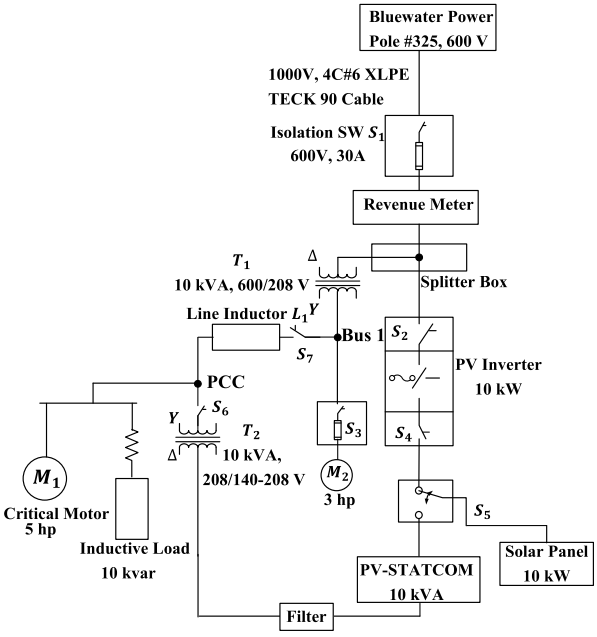

FIGURE 1. Schematic diagram of the study system at Bluewater Power Distribution Corporation, Sarnia, ON, Canada.

II. STUDY SYSTEM

The field demonstration of PV-STATCOM technology was conducted on the 10-kW grid-connected PV solar farm located on Confederation Street in the utility system of Bluewater Power Distribution Corporation, Sarnia, Ontario, Canada. The single line diagram of the study system and the photographs of the demonstration site are shown in Fig. 1 and 2, respectively. The photograph of the demonstration site for day and night time operation are shown in Fig 2 (a) and Fig. 2 (b), respectively. The PV solar farm is connected to Pole 325 using the switch S_1. Pole 325 in turn is connected through a 150kVA 600V/4.16kV transformer to the 4.16 kV distribution feeder 14F1 of Bluewater Power Distribution Corporation system, although not shown in Fig. 1. The voltage and current of the PV panels are 280V and 35.7A, respectively, for Maximum Power Point (MPP) operation. Solar power is fed to the grid using a commercial utility inverter rated 10kW, 600 V AC and 475V DC, operating at unity power factor. Switches S_2 and S_4 are used to isolate the existing PV inverter from the circuit. A 3-hp induction motor M_2 is used to operate the tracking system of the PV panels. This motor is connected to the 208V terminal of transformer T_1 (Bus 1) using switch S_3.

The utility inverter is controlled by its propertiary control provided by the manufacturer, and is not amenable to any modifications. For this reason, a separate three-phase two-level 10 kVA inverter controlled as PV-STATCOM is used for the field demonstration. This 10 kVA PV-STATCOM inverter includes six insulated gate bipolar transistors, gate drives, and protection circuit. The PV-STATCOM controller is designed in MATLAB/Simulink software and implemented on the dSPACE controller board. Current and voltage sensors are installed at the PV-STATCOM inverter and the load. The sensor signals are sent to the dSPACE controller board (DS1103) through ADC channels. The PV-STATCOM controller is implemented on the dSPACE controller board which generates appropriate firing pulses for the IGBT gates of the PV-STATCOM inverter based on the selected control objectives and operation mode. The Pulse Width Modulation (PWM) pulses generated from the dSPACE board are applied to the PV-STATCOM inverter interface panel through appropriate level shifter circuits. A graphical user interface (GUI) is designed in ControlDesk software to provide a control environment to supervise the PV-STATCOM system operation. A Yokogawa power analyzer (DL850E) is used to record various signals.

The PV-STATCOM inverter and the utility PV inverter are connected to the solar panels using a double-pole double-throw switch S_5. An LCL filter is used at the inverter terminal to filter out the switching harmonics and to maintain the THD of the inverter output within 5%. The filter inductance and capacitance are designed to be 1 mH and 100 μF, respectively [33]. As the MPPT voltage of PV panel is 280 V, a 140-208/208V intermediate transformer T_2 with 5% impedance is employed to connect the PV-STATCOM inverter to the utility transformer T_1.

In this field demonstration, the 10 kVA PV-STATCOM is used to stabilize a 5 hp induction motor M_1 during a major system disturbance. This large system disturbance is initiated by switching a 10 kvar inductive load. In this demonstration, a variable line inductor L_1 rated 5.1 mH in combination with the system short circuit reactance L_S at Pole #325 is used to vary the effective short circuit inductance of the grid, L_g, as seen by the PV-STATCOM. Switch S_7 is used to isolate the PV-STATCOM and load from the grid.

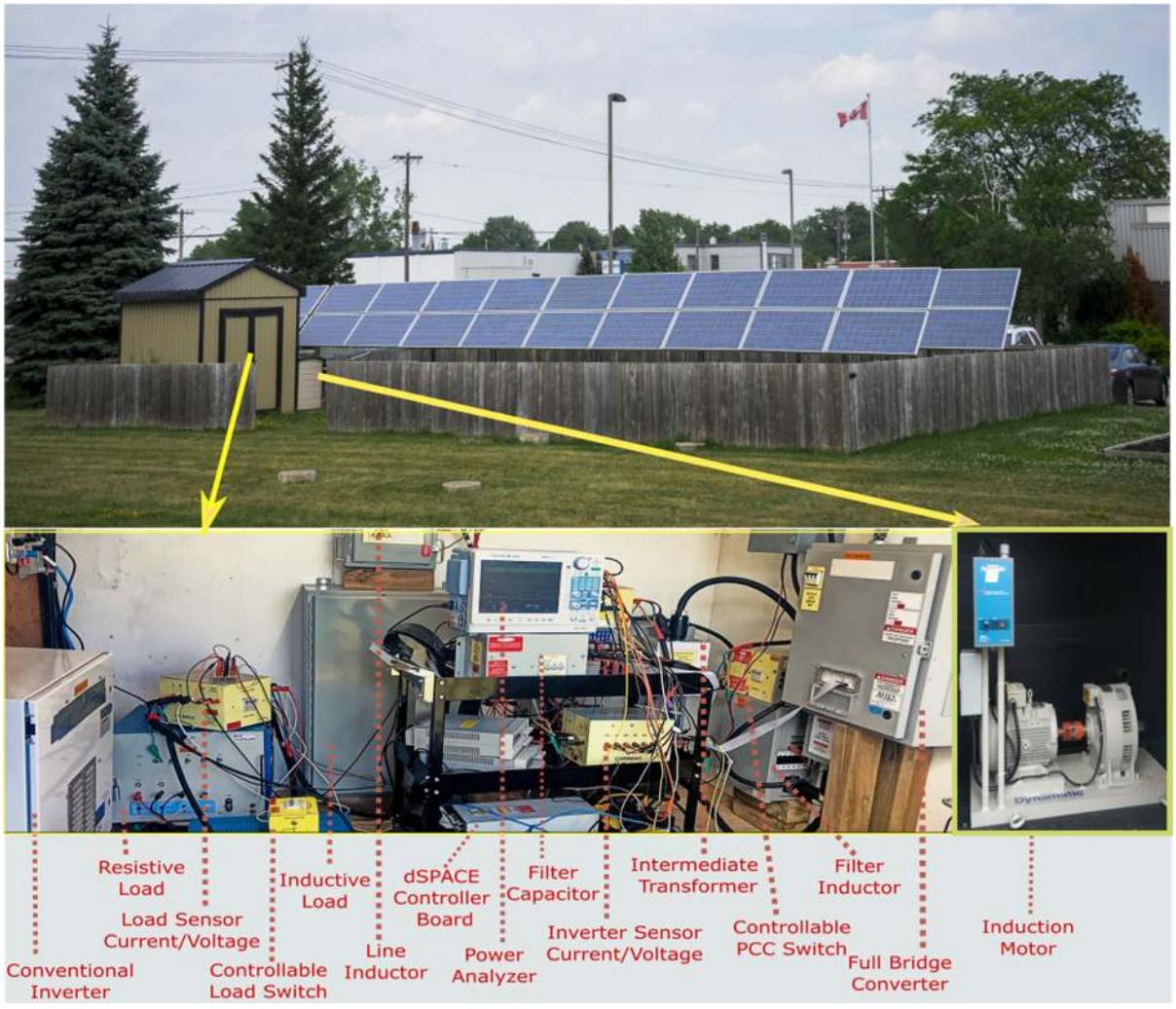

(a)

(b)

FIGURE 2. (a). Field implementation of PV-STATCOM at Bluewater Power Distribution Corporation, Sarnia, ON, Canada, (b). The PV-STATCOM field demonstration site during nighttime.

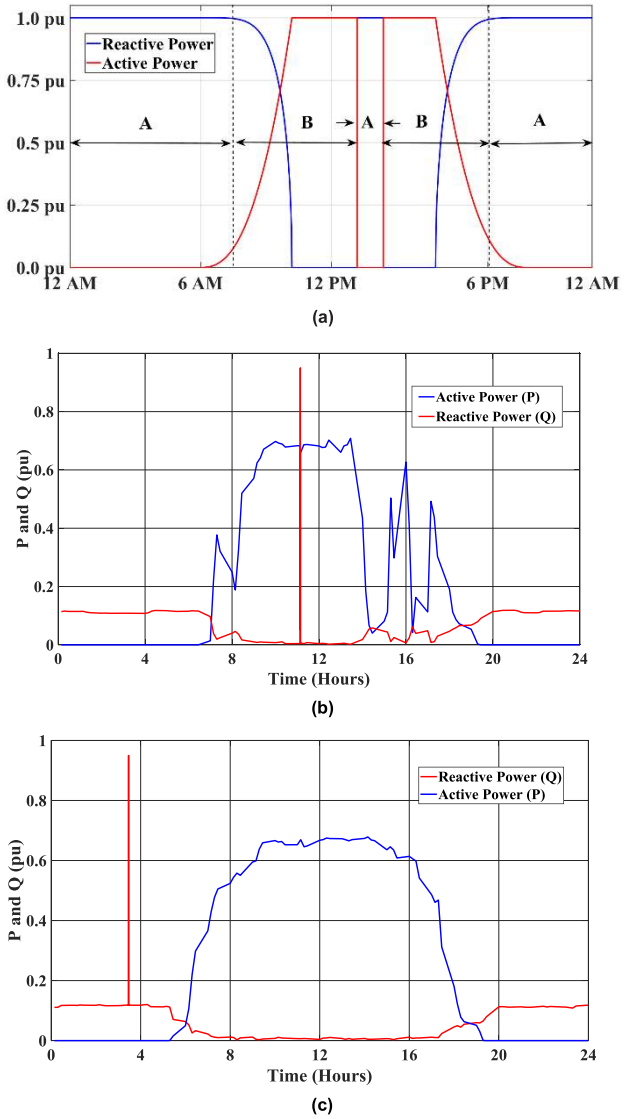

FIGURE 3. **(a). Typical active and reactive power exchange capability of PV-STATCOM during 24 hours on a sunny day; Regions A and B indicate Full STATCOM and Partial STATCOM modes of operation, respectively, (b). Active and reactive power output of the 10 kVA PV-STATCOM on June 2nd, 2019 (cloudy day), when it provided dynamic voltage control to stabilize the motor at 11.45 am. (c). Active and reactive power output of the 10 kVA PV-STATCOM on June 7th, 2019 (sunny day), when it provided dynamic voltage control to stabilize the motor at 3.30 am.**

For the nighttime operation of PV-STATCOM, the PV panels are disconnected from PV-STATCOM inverter using the switch S_5.

III. PV-STATCOM

Fig. 3 (a) shows the typical active/real power output and the reactive power exchange capability of a PV-STATCOM during 24 hour period on a sunny day. The different operating modes of PV-STATCOM are described below:

a) *Partial STATCOM*: In this mode, the available inverter capacity, i.e., inverter capacity remaining after real power generation during the daytime, is used for dynamic reactive power exchange with the grid as STATCOM. The active power production of the solar farm is not impacted at all.

b) *Full STATCOM:* In this mode, the active power output is curtailed autonomously, during any system stabilization need such as faults or disturbances, and the entire inverter capacity is made available for dynamic reactive power exchange with the grid as STATCOM.
Once the power system need for reactive support is fulfilled, the PV-STATCOM switches to active power generation at the pre-disturbance level. This mode is utilized during the daytime on a need basis, while it is fully available during nighttime.

c) *Full PV mode:* In this mode, the PV system generates maximum active power based on available solar irradiance, at unity power factor.

A. PERFORMANCE OF THE 10 kW PV PLANT WITH THE PROPOSED PV-STATCOM CONTROL

Figs. 3 (b) and (c) illustrate the real and reactive power outputs of the 10 kW PV solar farm on 2nd June (cloudy day) and 7th June 2019 (sunny day), respectively. A large system disturbance occurred on June 2nd at 11.45 am. The PV plant transformed into Full STATCOM and stabilized the IM. Also, on June 7th, the PV plant provided Full STATCOM operation during night at 3.30 am to stabilize the IM during the occurrence of a large system disturbance, as shown Fig. 3(c). The reactive power injection during Full STATCOM operation occurred over a duration of about 1.2s in both cases. This is indicated by the spike in reactive power in both Fig. 3 (b) and Fig. 3 (c).

The real and reactive power are measured at the secondary of the transformer T_1. Hence, the reactive power plotted in Figs. 3 (b) and (c) is the sum of the reactive power output of PV-STATCOM and the filter. The continuous 0.1 pu reactive power at night for both days is due to the reactive power output of filter capacitor. During day time, the reactive power consumed by the filter inductor increases with the increase in inverter current passing through it. Thus the measured reactive power reduces with increase in power output, as it is the resultant of reactive power generated by the capacitor and reactive power consumed by the inductor.

IV. PV-STATCOM CONTROLLER

Fig. 4 demonstrates the proposed PV-STATCOM control for the study system. The Thevenin's equivalent impedance of the feeder at pole 325 is represented as L_s and R_s.

The control objective is to use the solar system as PV-STATCOM to stabilize an induction motor during a major system disturbance. The different controller blocks within the overall PV-STATCOM control system are described below. The PV-STATCOM involves implementing additional controllers and novel control strategies on an existing PV solar system control. Fig. 4 therefore includes the novel controller blocks which relate exclusively to PV-STATCOM

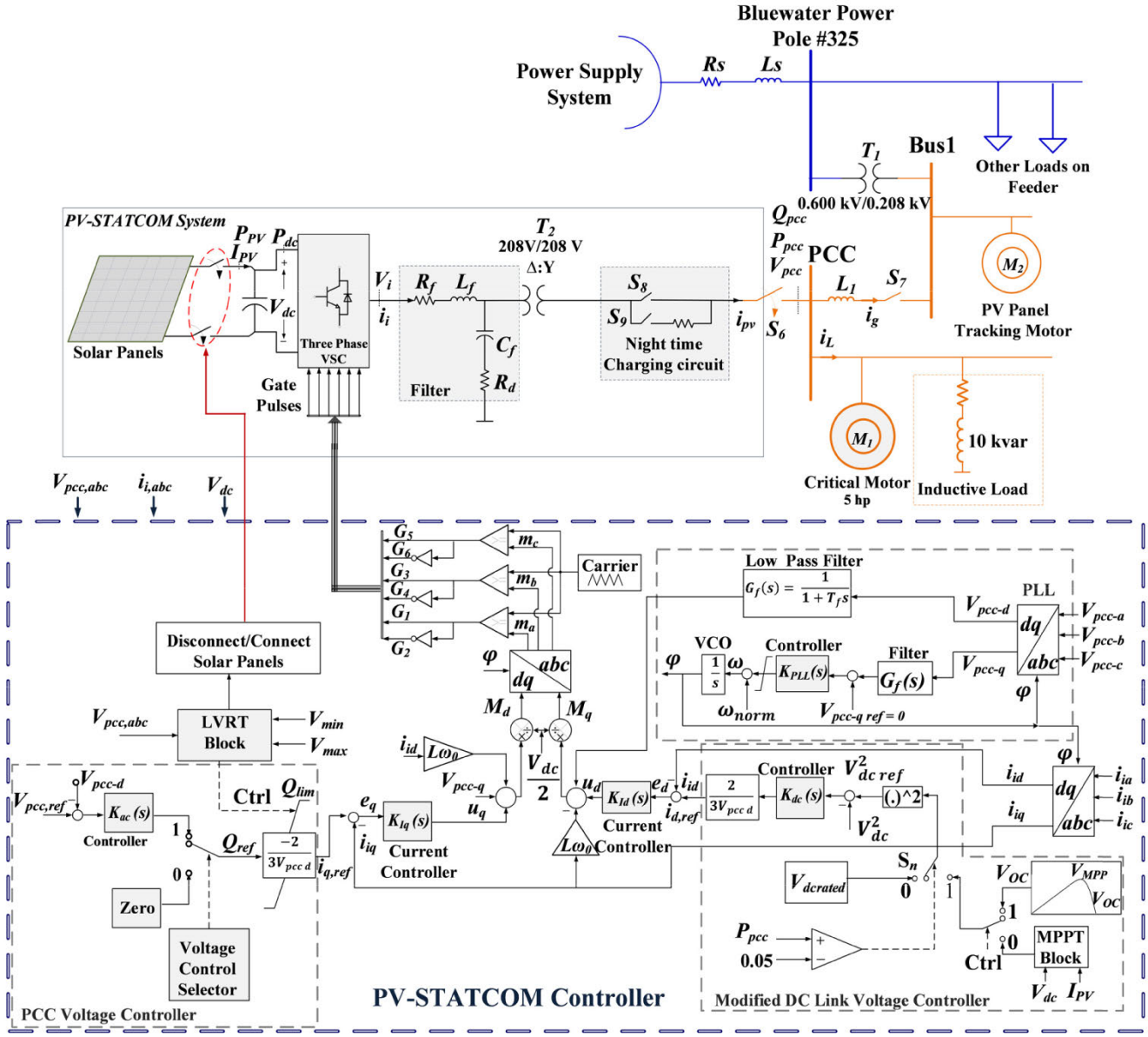

FIGURE 4. Single line diagram of a grid connected PV system with the proposed PV-STATCOM controller.

such as AC voltage controller, Low Voltage Ride Through (LVRT) block, Modified DC voltage controller, and an operating mode selector strategy. The other blocks such as PLL, *abc/dq* transformation block, current controllers, and PWM unit pertain to a conventional PV system controller, which are described here only for the sake of model completeness.

A. PHASE LOCKED LOOP (PLL)

The voltage and current vectors rotate with time-variant frequency $\omega(t)$ in *abc*-frame. The phase difference between the rotating voltage vector and stationary axes in *abc*-frame is defined by $\theta\,(t)$ The three-phase synchronous reference frame (SRF) PLL unit extracts the phase angle of PCC voltage for transforming the voltage and current signals from *abc*-frame to *dq*-frame and vice versa [33], [34]. The q-component of PCC voltage utilized in voltage control is given:

$$V_{pcc-q} = \hat{V} sin(\omega_0 t + \theta_0 - \varphi) \tag{1}$$

$$\frac{d\varphi}{dt} = \omega(t) \tag{2}$$

where, $\hat{V}$ is the amplitude of PCC phase voltage, ω_0 is system frequency and θ_0 is the initial phase angle of the AC system. Eqn. (1) reveals that for controlling the voltage angle at reference value $\varphi_{ref} = \omega_0 t + \theta_0$ the $q-$ component of voltage must regulated to zero ($V_{pcc-q} = 0$) [34].

In Fig. 4, a low pass filter is employed to reject high frequency harmonics of the voltage components. The filter transfer function is represented by $G_{filter}(s)$ where the filter time constant is $T_f = 1\ ms$. The Voltage-Controlled

Oscillator (VCO) block is a resettable integrator which converts frequency to phase angle. Hence, the compensated phase angle transfer function becomes:

$$\frac{d\varphi}{dt} = K_{pll}(t) \times G_{filter}(t) \times \hat{V} sin(\omega_0 t + \theta_0 - \varphi) \quad (3)$$

Since $(\omega_0 t + \theta_0 - \varphi)$ has a very small value, $sin(\omega_0 t + \theta_0 - \varphi)$ is considered equal to $(\omega_0 t + \theta_0 - \varphi)$. A proportional-integral (PI) controller is used to regulate V_{pcc-q} to 0. Subsequently, the open loop transfer function in the presence of the controller becomes:

$$H_{PLL}(s) = \frac{\hat{V} \times k_{PLL,gain}}{T_f} \left(\frac{s + z_{PLL}}{s + T_f^{-1}} \right) \frac{1}{s^2} \quad (4)$$

where $k_{PLL,gain}$ and z_{PLL} are PLL controller parameters. The "Symmetrical Optimum" technique is used to design the PI controller with the phase margin $\delta_m = 60°$ at cross over frequency $\omega_c = 268$ rad/s [33], [35].

B. CURRENT CONTROL

The active and reactive power outputs of PV-STATCOM system including the filter in dq-frame are [33], [34]:

$$P_s(t) = \frac{3}{2} \left(V_{pcc-d}(t) i_{pvd}(t) + V_{pcc-q}(t) i_{pvq}(t) \right) \quad (5)$$

$$Q_s(t) = \frac{3}{2} \left(-V_{pcc-d}(t) i_{pvq}(t) + V_{pcc-q}(t) i_{pvd}(t) \right) \quad (6)$$

where $V_{pcc-d}(t)$ and $V_{pcc-q}(t)$ are PCC voltages in dq-frame, and $i_{pvd}(t)$ and $i_{pvq}(t)$ are PV-STATCOM output currents in dq-frame. As the shunt filter current is very small, it can be assumed that PV-STATCOM current is almost equal to inverter current. Due to PLL operation, $V_{pcc-d} = |V|$ and $V_{pcc-q} = 0$. Consequently, in the utilized decoupled control, the real power output of the PV-STATCOM is controlled by i_{id} while reactive power output is controlled by i_{iq}, where i_{id} and i_{iq} are the inverter output currents in the dq-reference frame.

The inner control loops control currents wherein each loop receives the reference value from the outer control loop. For the active current, the reference value (i_{idref}) is the output of DC link voltage control. The reactive current reference (i_{iqref}) is determined by the AC voltage control or the Low Voltage Ride Through (LVRT) block. The reference values for current control loops are defined by the PV-STATCOM operation modes described later. The dynamics of the AC side of PV-STATCOM inverter are described as:

$$\vec{V}_i = R_f \vec{i_i} + L_f \frac{d\vec{i_i}}{dt} + \vec{V}_{pc} \quad (7)$$

For the two-level VSC constituting the PV-STATCOM with sinusoidal pulse width modulation (SPWM) the converter AC-side terminal voltage $V_{i,abc}$ is controlled as [33], [34]:

$$V_{i,abc} = \frac{V_{dc}}{2} m_{abc} \quad (8)$$

where V_{dc} and m_{abc} are DC bus voltage and modulation waveforms in the abc reference frame, respectively. Hence, PV-STATCOM inverter currents in dq-frame are [33]:

$$L_f \frac{di_{id}}{dt} = L_f \omega(t) i_{iq} - R_f i_{id} + \frac{V_{dc}}{2} M_d - V_{pcc-d} \quad (9)$$

$$L_f \frac{di_{iq}}{dt} = -L_f \omega(t) i_{id} - R_f i_{iq} + \frac{V_{dc}}{2} M_q - V_{pcc-q} \quad (10)$$

where, V_{dc} is the DC link voltage, M_{dq} are the modulation indices, $V_{pcc,dq}$ are PCC voltages, $i_{i,dq}$ are inverter currents and $V_{i,dq}$ are the voltages at AC side of PV-STATCOM inverter in dq frame, respectively.

The non-linear parts of (9) and (10) are added as feed-forward terms to linearize the equations:

$$L_f \frac{di_{id}}{dt} + R_f i_{id} = u_d \quad (11)$$

$$L_f \frac{di_{iq}}{dt} + R_f i_{iq} = u_q \quad (12)$$

where u_d and u_q are input control signals which controls i_{id} and i_{iq} individually. The sum of control signals and feed-forward terms generates the modulation indices as below:

$$M_d = \frac{2}{V_{dc}} \left(u_d - L_f \omega_0 i_{iq} + V_{pcc-d} \right) \quad (13)$$

$$M_q = \frac{2}{V_{dc}} \left(u_q + L_f \omega_0 i_{id} + V_{pcc-q} \right) \quad (14)$$

After transforming to abc-frame, the modulation indices are compared with the carrier signal to generate the IGBT gate pulses. To achieve faster response time and zero steady-state error, a PI controller is used for each current component. The parameters of PI controllers are calculated as [33]:

$$K_{I,dq}(s) = \frac{k_{p,dq} s + k_{I,dq}}{s} \quad (15)$$

$$k_{p,dq} = \frac{L_f}{\sigma_{i,dq}} \quad (16)$$

$$k_{I,dq} = \frac{R_f}{\sigma_{i,dq}} \quad (17)$$

where $\sigma_{i,dq}$ is the time constant for d-control and q-control loops to shift the transfer function pole. The time constant for both loops is chosen 1 ms.

C. MODIFIED DC LINK VOLTAGE CONTROLLER

By ignoring losses in the inverter and filter circuit, the DC side power of the inverter P_{dc} can be considered equal to the power on AC side of PV-STATCOM inverter P_{pcc}, as below:

$$P_{dc} \approx P_{pcc} = \frac{3}{2} V_{pcc-d} i_{pvd} \quad (18)$$

The power balance at the DC side of the PV-STATCOM inverter is given by:

$$P_{PV} = P_{dc-cap} + P_{dc} \quad (19)$$

where P_{PV}, P_{dc-cap} and P_{dc} are PV panel power, DC-link capacitor power and DC side power of the VSC. The DC

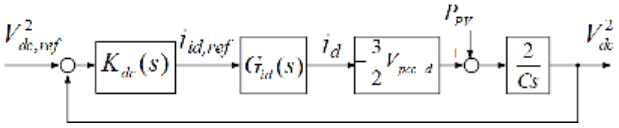

FIGURE 5. Block diagram of DC-bus voltage controller.

power output of the solar panel is calculated by a non-linear function as below:

$$P_{PV} = f(RTV_{dc}) = n_p I_{sc} V_{dc} - n_p I_0 V_{dc} \left[e^{\left(\frac{qV_{dc}}{kTn_s}\right)} - 1 \right] \quad (20)$$

where, I_0 is the diode saturation current, electron charge $q = 1.6e^{-19}$ coulomb, T is the cell temperature, $k = 1.38e^{-23}$ is the Boltzmann's constant, while n_s and n_p are the number of series and parallel cells.

By substituting (18) and (20) in (19) and considering active current transfer function:

$$\frac{d}{dt}\left(V_{dc}^2\right) = \frac{2}{C}\left(f(R, T, V_{dc}) - \frac{3}{2}V_{pcc-d}\left(G_{id}(t)\right) i_{id,ref}\right) \quad (21)$$

where $G_{id}(s)$ is the transfer function of closed-loop active current loop. To use linear control method, the non-linear solar power output of solar panel is added as a feed-forward term to compensate its effect [36]. Hence, the open-loop transfer function of DC voltage control is simplified to:

$$G_{dc}(s) = \frac{V_{dc}^2}{i_{id,ref}} = -\frac{3}{C}V_{pcc-d}\frac{1}{s(\sigma_{i,d}s + 1)} \quad (22)$$

It should be noted that in Full STATCOM mode, the solar panel power is zero. The uncompensated DC link voltage control is unstable, and hence a PI controller is added to regulate the DC link voltage to the reference value. Fig. 5 illustrates the block diagram of DC voltage control loop. The compensated open loop transfer function is transformed to:

$$\begin{aligned} H_{dc}(s) &= K_{dc}(s) \times G_{dc}(s) \\ &= -\frac{3 \times V_{pcc-d} \times k_{dc,gain}}{2 \times \sigma_{i,d}}\left(\frac{s + z_{dc}}{s + \sigma_{i,d}^{-1}}\right)\frac{1}{s^2} \end{aligned} \quad (23)$$

where $\boldsymbol{k_{dc,gain}}$ and $\boldsymbol{z_{dc}}$ are the parameters of DC link voltage controller. Due to the two poles at origin, the Symmetrical Optimum technique [35] is used to design this controller with phase margin $\delta m = 50°$ at cross over frequency $\omega c = 364$ rad/s. It should be noted that the dynamics of DC voltage control is slower than active current control loop.

Intelligent controllers can be also used for DC link voltage control. However, for this PV-STATCOM demonstration project, since the objective is to only demonstrate a novel concept of using solar farm as a STATCOM, a simple control is used.

D. MODIFICATIONS FOR PV-STATCOM OPERATION

In a conventional PV system, the DC link reference voltage ($V_{dc,ref}$) is provided by the MPPT module. In the proposed PV-STATCOM operation, the controller curtails active power generation during a disturbance and uses the entire inverter capacity to exchange (inject/absorb) reactive power. This objective is achieved by setting $V_{dc,ref}$ to open circuit voltage V_{oc} of the solar panels at which voltage the power output of the PV panels reduces to zero. Once, the system returns to stable operation, the PV-STATCOM controller ramps up active power to the maximum available power per available irradiance. The power is ramped up by varying $V_{dc,ref}$ from the open circuit voltage V_{oc} to the voltage corresponding to the maximum power point V_{MPP}.

It is noted that during the daytime, when the sun is available, the DC voltage control uses solar power to compensate the inverter switching losses, and thereby keep the DC link capacitor charged to the desired voltage reference level. However, during nighttime, the DC voltage reference is switched to a constant value $V_{dcrated}$ by switch S_n The required active power for compensating switching losses (1-3%) and for maintaining DC voltage at the reference value $V_{dcrated}$ is provided from the grid, as in STATCOMs [1], [2].

E. PCC VOLTAGE CONTROL

The PCC voltage in *abc*-frame is given below:

$$V_{pcc,abc} = L_g\frac{di_{g,abc}}{dt} + V_{g,abc} \quad (24)$$

where $V_{pcc,abc}$ is PCC voltage, $i_{g,abc}$ is grid current, L_g is the inductive component of effective short circuit impedance of grid as viewed from PCC and $V_{g,abc}$ is grid voltage in *abc*-frame. The PCC voltage magnitude is expressed only by V_{pcc-d} since V_{pcc-q} is controlled to zero by the PLL controller. Therefore, the PCC voltage is given by:

$$\begin{aligned} V_{pcc-d} &= -L_g\omega_0 i_{gq} + L_g\frac{di_{gd}}{dt} + \hat{V} \\ \text{where, } L_g &= L_s + L_1 \end{aligned} \quad (25)$$

Neglecting the current of the shunt filter capacitor,

$$i_{g,dq} = i_{L,dq} - i_{i,dq} \quad (26)$$

where, $i_{L,dq}$ are load current components in $d-q$ the frame. By substituting (26) in (25):

$$V_{pcc-d} = -L_g\omega_0 i_{iq} + L_g\omega_0 i_{Lq} - L_g\frac{di_{id}}{dt} + L_g\frac{di_{Ld}}{dt} + \hat{V} \quad (27)$$

The uncompensated transfer function of voltage control based on i_{iq} is given by:

$$G_{ac}(s) = G_{iq}(s) \times \left(-L_g\omega_0\right) = \frac{-L_g\omega_0}{1 + \sigma_{i,q}s} \quad (28)$$

where $G_{iq}(s)$ is the transfer function of closed-loop reactive current loop. The other terms of (27) are added as feed-forward terms. Due to negative gain, the uncompensated loop of AC voltage loop is unstable. Fig. 6 demonstrates the equivalent PCC voltage control with an Integral controller to regulate the PCC voltage at reference value and increase stability margin.

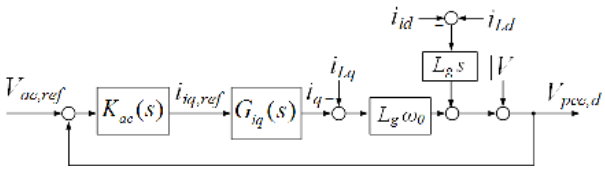

FIGURE 6. Block diagram of PCC voltage controller.

The open loop transfer function of the compensated voltage controller is expressed as:

$$H_{ac}(s) = \frac{k_{gain,ac}}{s} \times G_{iq}(s) \times \left(-L_g\omega_0\right) = \frac{-L_g\omega_0 k_{gain,ac}}{s(1+\sigma_{i,q}s)} \quad (29)$$

The closed-loop bandwidth of the PCC voltage loop is designed to be $\omega_{c,AC} = 100\text{rad/s}$ which is 10 times smaller than reactive current control loop [33], [34].

F. MODIFICATIONS FOR PV-STATCOM OPERATION

The ''Voltage Control Selector'', as shown in Fig. 4, determines if the solar farm is expected to provide voltage control. If voltage control is selected, the reactive power reference Q_{ref} is taken to be the output of the controller K_{ac}.

Voltage control can be performed in two modes: Partial STATCOM or Full STATCOM.

The PV-STATCOM reactive power output Q_{inv} is given by:

$$Q_{inv} = Q_{pcc} - \omega_0 * C_f V_{pcc}^2 + \omega_0 * L_f i_i^2 \quad (30)$$

In Partial STATCOM mode the PV-STATCOM reactive power output Q_{inv} is controlled within an upper limit Q_{lim} equal to Q_{rem}, i.e. the inverter capacity remaining after active power generation at that time instant of the day. In Full STATCOM mode Q_{inv} is controlled within an upper limit Q_{lim} equal to S_{inv}, i.e. the full rating of the inverter, during day or night. If voltage control function is not selected, as in Full PV mode of operation, Q_{ref} is set to zero. The limit Q_{lim} is determined by the LVRT block and ''Operation Mode Selector'' as described below.

G. LOW VOLTAGE RIDE THROUGH (LVRT) BLOCK

During a voltage swell or sag, the LVRT block activates PV-STATCOM operation. The voltage limits are set at 0.95 pu and 1.05, respectively, for detecting voltage sag and swell based on LVRT/HVRT criterion of Independent Electricity System Operator (IESO), Ontario. If a voltage disturbance is detected, the active power is curtailed autonomously, and the entire inverter capacity is made available for dynamic reactive power support to operate the PV inverter in Full STATCOM mode. Fig. 7 illustrates the LVRT control loop with an Integral controller ($K_{Vac-LVRT}$) to regulate the PCC voltage at the pre-disturbance value. As shown, the pre-disturbance value is limited in the acceptable range, between 0.95 pu and 1.05 pu. The LVRT block consists of a voltage controller with a higher bandwidth, lower phase margin and a different current limit as compared to normal voltage controller. Hence, the controller is able to track the reference command faster with higher

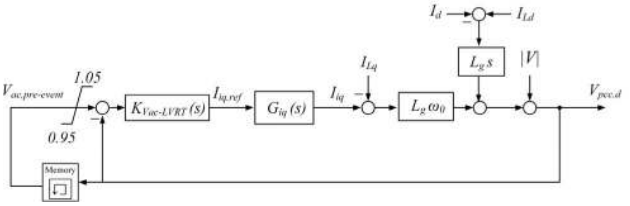

FIGURE 7. Block diagram of the LVRT controller.

reactive power support. The closed-loop bandwidth of LVRT control is designed to be $\omega_{c,LVRT} = 364\text{rad/s}$ with phase margin of $\delta_{LVRT} = 50°$ [33], [35].

The MPPT control is used for conventional PV solar power generation [34]. It determines the reference value for DC link voltage control to generate maximum power from the solar panel based on available solar irradiance [34]. However, MPPT control is not required for PV-STATCOM operation. During LVRT event, the control system regulates the DC voltage at open source voltage of solar panel to reduce its active power output to zero. In other words, the MPPT block will be bypassed during LVRT event. Hence, performance of MPPT algorithm does not impact the effectiveness of LVRT control.

H. IMPLEMENTATION OF NIGHTTIME OPERATION OF PV-STATCOM

The nighttime operating condition is achieved by two mechanisms:

i) During initial PV-STATCOM testing studies, the night time operation is emulated during the day by mimicking the night time condition for the inverter. For this, the PV panel is disconnected from the PV-STATCOM inverter using switch S_5. As PV panels are disconnected from the inverter, the inverter does not inject any active power into the grid and remains idle, similar to its behaviour during nighttime.

ii) For actual nighttime PV-STATCOM operation, certain modifications are made in the PV-STATCOM control. Since at night the DC input power to the PV inverter is zero, the DC link capacitor is charged from the grid using a ''Nighttime Charging circuit'' utilizing the diodes across the IGBT switches of the inverter. The charging circuit consists of a resistor which is used to limit the inrush current during charging, as depicted in Fig. 4. Switch S_9 is kept ON while switch S_8 is turned OFF for nighttime charging. Once the DC link capacitor is charged, the charging circuit is disabled to prevent losses in the charging circuit, by turning the switch S_8 ON, and S_9 OFF. Thereafter, the DC voltage reference is switched by S_n to the constant value $V_{dcrated}$ for STATCOM operation.

V. OPERATION MODE SELECTOR

Fig. 8 demonstrates the flowchart of the PV-STATCOM control with different operating modes during nighttime and daytime. In Fig. 8, V_{L1} and V_{H1} are the utility limits for low and high voltage operation, respectively. V_{L2} and V_{H2} are Low and High Voltage Ride Through (L/HVRT) limits, respectively. For this study system the utility voltages

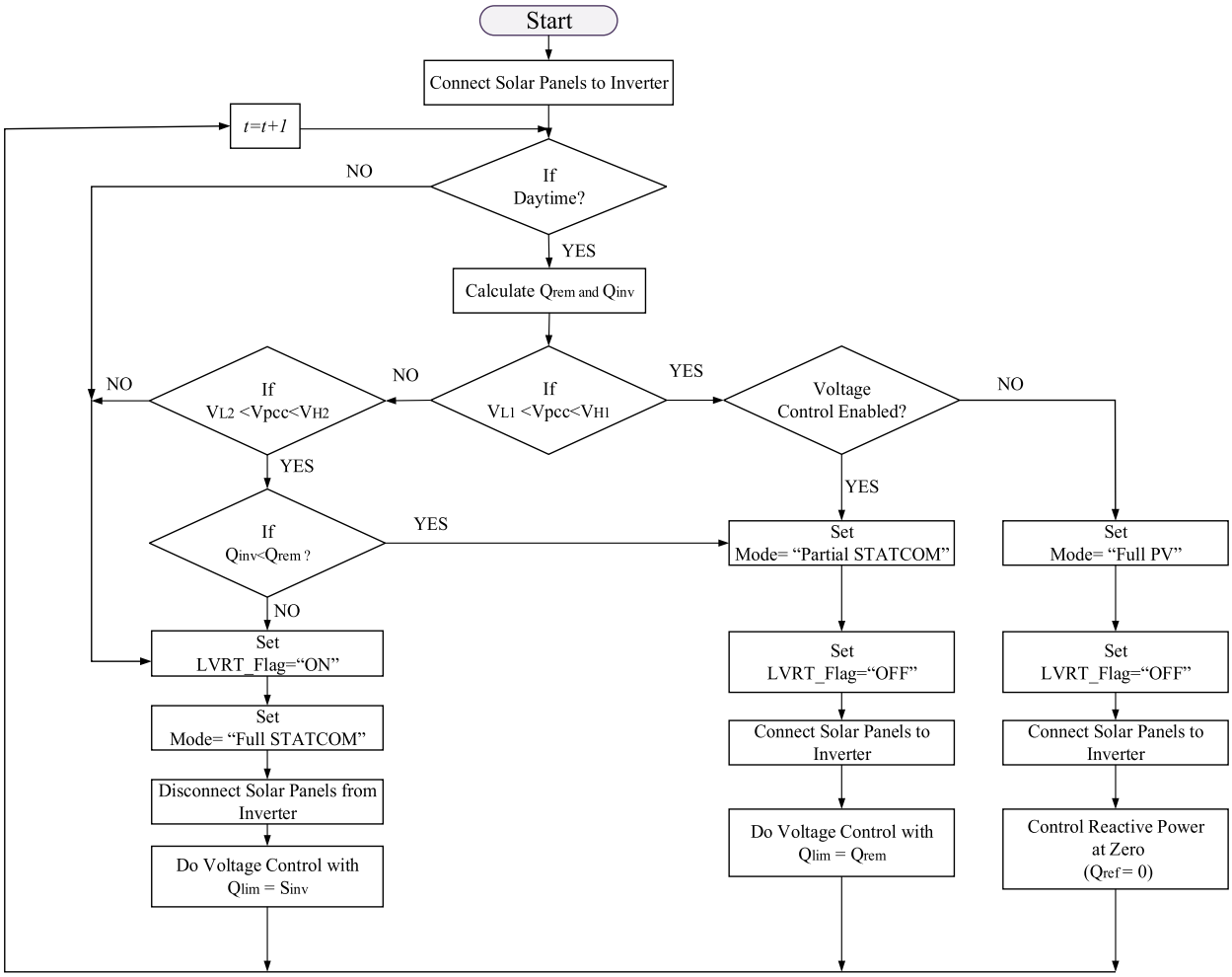

FIGURE 8. Flowchart of the PV-STATCOM operating modes.

limits V_{L1} and V_{H1} are selected to be 0.95 pu and 1.05 pu, respectively [20]. Correspondingly, the L/HVRT limits V_{L2} and V_{H2} are considered to be 0.90 pu and 1.10 pu, respectively [20].

During daytime, if PCC voltage is within the acceptable range of utility limits, and if the solar farm is not intended to provide ''voltage control'', Full PV mode is chosen as the mode of operation. In this mode, the solar panels are connected to the inverter and reactive power reference Q_{ref} is set to zero. The PV system then utilizes the inverter only for active power generation.

However, if the solar farm is expected to provide ''voltage control'', the voltage is controlled utilizing Partial STATCOM mode. If the voltage is out of utility limits but within the L/HVRT limits, the controller uses the remaining reactive power (Q_{rem}) in the Partial STATCOM mode to regulate PCC voltage. In this case $Q_{lim} = Q_{rem}$.

If the voltage is out of L/HVRT limit range or if the remaining capacity of the inverter is insufficient for voltage control, the controller disables active power from solar panels and allocates the entire inverter capacity (S_{inv}) for reactive power support. At this time, $Q_{lim} = S_{inv}$. After the L/HVRT event is cleared, if the voltage is successfully regulated to within the utility specified range, the operation mode is reset to Partial STATCOM mode for voltage control with active power enabled from solar panels.

During nighttime, only Full STATCOM mode is used for voltage control, and hence the entire inverter capacity is utilized for dynamic reactive power exchange.

VI. FIELD DEMONSTRATION RESULTS

The first-time field demonstration of the PV-STATCOM was performed on 16th December 2016. The PV-STATCOM is still connected to the system and studies are ongoing with newer controls. This paper, however, presents the results for the first field demonstration of utilizing the PV solar farm as PV-STATCOM for stabilizing a critical induction motor during nighttime and daytime.

A. RESPONSE OF CONVENTIONAL PV INVERTER FOR LARGE DISTURBANCE DURING DAY TIME

A large system disturbance is simulated by switching a 10 kvar inductive load at PCC during day time for a period of 1.2s, without the PV-STATCOM controller activated.

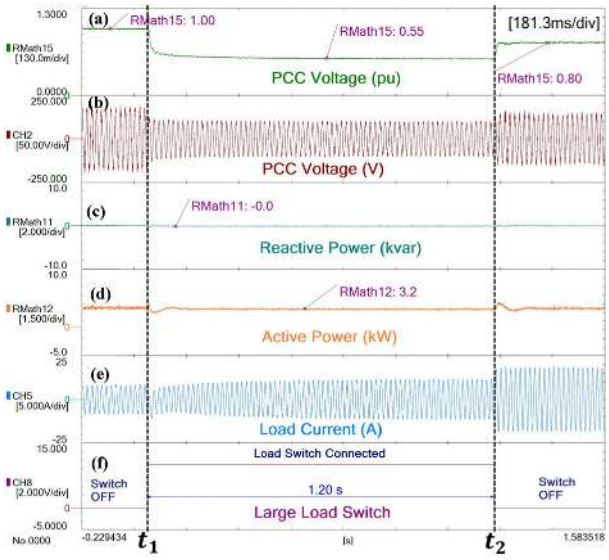

FIGURE 9. Response of the conventional PV inverter for large load switching during day time without PV-STATCOM controller.

The responses of PV solar farm in Full PV mode and the induction motor for this scenario are depicted in Fig. 9.

Figs. 9 (a)-(f) illustrate the PCC rms voltage (pu), PCC instantaneous voltage (V), Reactive power output of the inverter (kvar), Active power output of the inverter (kW), Motor current (A) and status of the large load switch, respectively.

$t < t_1$: The PCC voltage is 1 pu during this time interval. The inverter is operating at unity power factor by injecting the maximum available active power of 3.2 kW to the grid and keeping reactive power at zero. The motor is operating at steady state by providing the required load torque by consuming 8A.

$t = t_1$: A disturbance is created by connecting 10 kvar inductor to the PCC. Due to this large load switching, the PCC voltage drops to a low value of 0.55 pu. Since the inverter is operating at unity power factor, the inverter continues injecting 3.2 kW active power to the grid while maintaining its reactive power output at zero. Due to the voltage drop, the motor starts consuming a large reactive power and the motor current increases to 12 A.

$t = t_2$: The large load is disconnected and the voltage starts recovering. However, due to inadequate reactive power support, the motor continues consuming a higher current of 16 A. Due to the large motor current, the PCC voltage recovers to 0.8 pu only. The motor eventually stalls.

This study shows that the induction motor will become unstable and stall during a large disturbance in the absence of any dynamic reactive power support from the solar farm.

B. RESPONSE OF PV-STATCOM FOR LARGE DISTURBANCE DURING DAY TIME

The PV-STATCOM control is now enabled on the solar farm. The PV-STATCOM inverter and induction motor response for

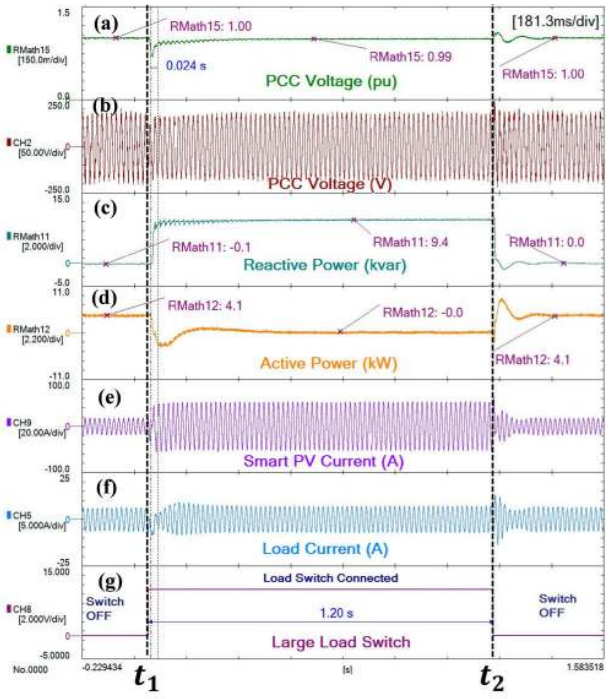

FIGURE 10. Response of the PV-STATCOM for large load switching during day time with PV-STATCOM controller.

the same large load switching at PCC for a period of 1.2s during day time with PV-STATCOM controller are shown in Fig. 10.

Figs. 10 (a) - (g) illustrate the PCC rms voltage (pu), PCC instantaneous voltage (V), Reactive power output of the PV-STATCOM inverter (kvar), Active power output of the PV-STATCOM (kW), PV-STATCOM inverter current (i_{pv})(A), Motor current (A) and status of the large load switch, respectively.

$t < t_1$: The PV-STATCOM is operating at unity power factor by generating 4.1 kW power.

$t = t_1$: The large load is connected and consequently, the system voltage drops to 0.65 pu. The PV-STATCOM detects the drop in the voltage and autonomously switches to Full STATCOM mode. In this mode, the active power is curtailed, and full inverter capacity is utilized for injecting reactive power. The PV-STATCOM inverter reduces its active power from 4.1 kW to zero and injects 9.4 kvar reactive power within 0.024 sec (approximately 1.4 cycle). The fast reactive power injection is able to bring the PCC voltage to 0.99 pu and thus prevent the motor from stalling.

$t = t_2$: The large load is disconnected at $t = t_2$. The controller detects it and switches to Full PV mode. The reactive power output is reduced to zero and active power is ramped up to 4.1 kW. The motor continues stable operation and consumes its pre-disturbance current of 8 A.

This study demonstrates that the PV-STATCOM is able to inject almost 1 pu reactive current within 1.4 cycles. This response time matches that of commercial STATCOMs [1], [2]. The rapid reactive power support by PV-STATCOM

successfully prevents motor instability during a large disturbance. It is further demonstrated that the PV-STATCOM control is able to ramp the active power to its pre-disturbance level within 3 cycles after the large load is disconnected.

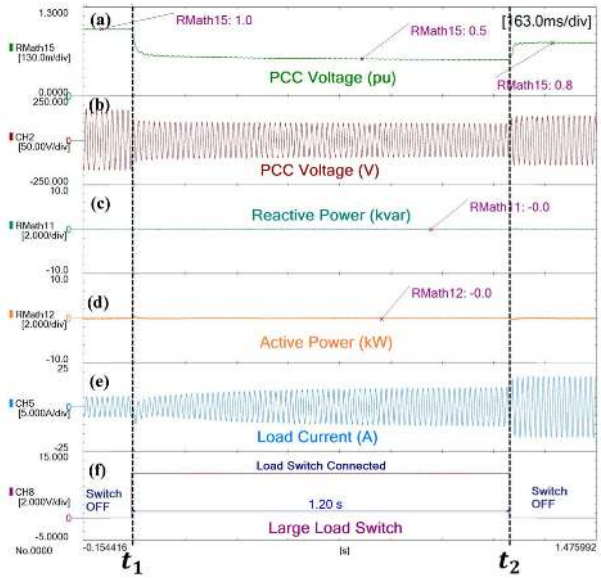

FIGURE 11. Response of the conventional PV inverter for large load switching during night time.

C. RESPONSE OF CONVENTIONAL INVERTER FOR LARGE DISTURBANCE DURING NIGHTTIME

Studies are now performed during nighttime. The responses of the PV solar farm and the induction motor for the switching of 10 kvar inductor at PCC during nighttime, for a period of 1.2s, without PV-STATCOM controller are shown in Fig. 11.

Figs. 11 (a) - (f) illustrate the PCC rms voltage (pu), PCC instantaneous voltage (V), Reactive power output of the inverter (kvar), Active power output of the inverter (kW), Motor current (A) and status of the large load switch, respectively.

$t < t_1$: The inverter is idle as solar power is zero at night. The motor is operating at steady state by providing the required load torque, by drawing power from the grid.

$t = t_1$: A large disturbance is created by connecting 10 kvar inductor to the PCC. Due to this large load switching, the PCC voltage drops to 0.5 pu. Due to this large voltage drop, the motor starts consuming a high amount of reactive power and the motor current increases to 12 A.

$t = t_2$: The large load is disconnected, due to which the voltage starts recovering but only up to 0.8 pu. Since no reactive power support is available the motor consumes a larger current of 16 A and eventually stalls.

This study demonstrates that the induction motor will become unstable and stall during a large disturbance at night when no reactive power support is available.

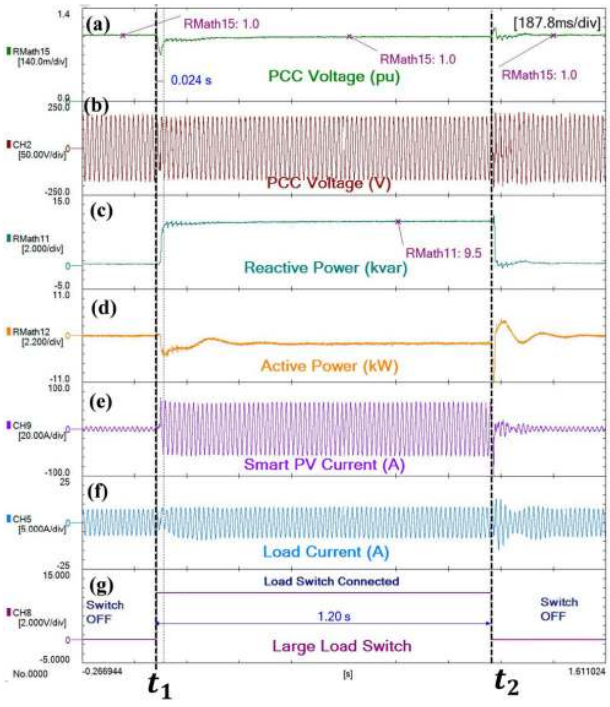

FIGURE 12. Response of the PV-STATCOM for large load switching during night time.

D. RESPONSE OF PV-STATCOM FOR LARGE DISTURBANCE DURING NIGHTTIME

Studies are conducted during nighttime with the PV-STATCOM control activated. The PV-STATCOM inverter and induction motor responses for the large load switching at PCC during night time, for a period of 1.2s, with PV-STATCOM controller are shown in Fig. 12.

Figs. 12 (a) - (g) illustrate the PCC rms voltage (pu), PCC instantaneous voltage (V), Reactive power output of the PV-STATCOM inverter (kvar), Active power output of the PV-STATCOM (kW), PV-STATCOM inverter current (i_{pv})(A), Motor current (A) and status of the large load switch, respectively.

$t < t_1$: The system is operating in a steady state condition with a PCC voltage of 1 pu. The PV-STATCOM is idle. The motor is providing the load torque by consuming 8 A from the grid.

$t = t_1$: The large load is connected and as a consequence, the bus voltage drops to 0.65 pu. The PV-STATCOM detects the drop in the voltage and switches to Full STATCOM operation. In this mode, the full inverter capacity is utilized for injecting reactive power. The PV-STATCOM inverter injects 9.4 kvar reactive power. The speed of response for the controller is seen to be 1.4 cycle. This fast reactive power injection is able to bring the PCC voltage to 0.99 pu and thus prevent the motor from stalling.

$t = t_2$: The large load is disconnected at $t = t_2$. The controller detects it and ceases reactive power injection. The motor continues to operate in a stable manner with its pre-disturbance current level of 8 A.

This study demonstrates that fast dynamic reactive power support by PV solar farm with the proposed PV-STATCOM control can prevent motor instability during large disturbance at nighttime, when conventional PV solar farms are usually dormant.

VII. CONCLUSION

This paper presents the first stage results of the first in Canada (and first in the world, to the best of authors' knowledge) field demonstration of a novel PV solar farm control as a STATCOM, termed PV-STATCOM. This new control is demonstrated on a 10 kW PV solar farm installed in the utility network of Bluewater Power Distribution Corporation, Sarnia, ON, for stabilizing a critical 5 hp induction motor both during night and day. The motor and the PV solar farm are connected at the same bus (PCC). A large disturbance is initiated by switching a 10 kvar inductive load at PCC, both during night and day. Following are the conclusions of the field studies:

1) The switching of large inductive load causes a drop in the PCC voltage to about 0.5 pu both during night and day. The motor becomes unstable and stalls in both cases.

2) The PV-STATCOM control on the solar farm successfully ensures stable operation of the motor. The motor continues to operate in a stable manner despite the switching of the large load both during night and day.

3) The PV-STATCOM regulates the voltage to 1 pu in about 1.4 cycles, both during night and day. This speed of response is identical to actual STATCOMs

4) During daytime, the PV-STATCOM further restores the active power generation of the solar farm from zero to its pre-disturbance level in less than 3 cycles after the large load is switched off.

The PV-STATCOM is thus shown to be a new smart inverter, which:

1) provides dynamic voltage control in 1-2 cycles, whereas the present smart inverters provide voltage control (volt-var or volt-watt) in 1-3 seconds [20], and

2) provides dynamic voltage control at night, which conventional smart inverters do not [20].

The PV-STATCOM is further a new FACTS device, which:

1) provides dynamic voltage control with a similar rapid response as a STATCOM [1], [2], and

2) is about 50 times lower cost than an equivalent sized STATCOM (or SVC).

A solar farm mainly comprises: i) PV modules, ii) Voltage source converters (VSCs) i.e., inverters, and iii) its associated electrical/civil infrastructure (substation, transformer, switchgear, buswork, protection systems, etc). On the other hand, an equivalent sized STATCOM essentially consists of: i) VSCs and ii) its associated electrical/civil infrastructure which is quite similar to that of a PV solar farm. It is noted that for a PV solar plant the cost of VSCs hardware and their control system is about 5-8% of the entire plant cost. Furthermore, the cost of PV solar plant level controls is only about 1% of total PV plant cost. Now, if a utility has identified the need for installing a STATCOM for a dynamic voltage control application, and if an equivalent size PV solar farm is available nearby, only an additional PV-STATCOM controller with its measurement circuitry needs to be augmented to the existing solar farm VSCs and their controls to transform it into a STATCOM. This additional expense is very small and therefore makes PV-STATCOM almost 50 times more economical than an equivalent sized STATCOM.

With the unprecedented growth of PV solar farms worldwide, it is quite likely that solar farms may find themselves installed in the vicinity of critical induction motors. This novel functionality of solar farms as PV-STATCOM can enable such solar farms to provide a stabilization service to the critical motors on a 24/7 basis at a far lower cost than STATCOMs and SVCs that are normally used to stabilize such critical motors. Such functionality can therefore open up a new revenue stream for solar farms in addition to the sale of active power.

WORK IN PROGRESS

The utility demonstration project is ongoing. Coordinated active and reactive power controls have been implemented on the PV-STATCOM and their effectiveness is being tested on 15 km remotely located critical motor considering signal communication delays, etc. Results of these ongoing studies will be presented in a subsequent paper.

This pioneering work has motivated several research studies internationally. For instance, in 2017, NREL, published a report on demonstrating essential reliability services by a 300-MW solar photovoltaic plant, in which it is stated that, "…Future plans by the project team include:… 'Demonstrating true PV STATCOM functionality during nighttime hours…'" [37].

REFERENCES

[1] N. G. Hingorani, L. Gyugyi, *Understanding FACTS*. Piscataway, NJ, USA: IEEE Press, 1999.
[2] R. M. Mathur and R. K. Varma, *Thyristor-Based FACTS Controllers for Electrical Transmission Systems*. Hoboken, NJ, USA: Wiley, 2002.
[3] T. Ackermann, *Wind Power in Power Systems*, 2nd ed. Hoboken, NJ, USA: Wiley, 2012.
[4] D. A. Jarc and J. D. Robechek, "Static induction motor drive capabilities for the petroleum industry," *IEEE Trans. Ind. Appl.*, vol. IA-18, no. 1, pp. 41–45, Jan. 1982.
[5] R. Bristow, "Induction motors and their controllers as part of energy reduction strategies within the pulp & paper industry," *Paper Technol.*, vol. 44, no. 7, pp. 25–35, 2003.
[6] J. C. Gomez, "Behavior of induction motor due to voltage sags and short interruptions," *IEEE Trans. Power Del.*, vol. 17, no. 2, pp. 434–440, Apr. 2002.
[7] E. G. Potamianakis and C. D. Vournas, "Short-term voltage instability: Effects on synchronous and induction machines," *IEEE Trans. Power Syst.*, vol. 21, no. 2, pp. 791–798, May 2006.
[8] O. V. Thorsen and M. Dalva, "A survey of faults on induction motors in offshore oil industry, petrochemical industry, gas terminals, and oil refineries," *IEEE Trans. Ind. Appl.*, vol. 31, no. 5, pp. 1186–1196, Sep. 1995.
[9] EPRI, "The cost of power disturbances to industrial & digital companies," Electr. Power Res. Inst., Palo Alto, CA, USA, Tech. Rep. 3002000476, Aug. 2012.
[10] A. E. Hammad and M. Z. El-Sadek, "Prevention of transient voltage instabilities due to induction motor loads by static VAr compensators," *IEEE Trans. Power Syst.*, vol. 4, no. 3, pp. 1182–1190, Aug. 1989.

[11] O. T. Tan and R. Thottappillil, "Static VAr compensators for critical synchronous motor loads during voltage dips," *IEEE Trans. Power Syst.*, vol. 9, no. 3, pp. 1517–1523, Aug. 1994.
[12] M. Ebadian and M. Alizadeh, "Effect of static VAR compensator to improve an induction motor's performance," in *Proc. Conf. IPEC*, Singapore, Oct. 2010, pp. 209–214.
[13] M. Hedayati and N. Mariun, "Assessment of different voltage sags on performance of induction motors operated with shunt FACTS," in *Proc. 3rd Power Electron. Drive Syst. Technol.*, Feb. 2012, pp. 483–489.
[14] *VarPro STATCOM Dynamic Reactive Power Compensation Power Quality Solutions for Heavy Industry*, ABB, New Berlin, WI, USA, 2015.
[15] *STATCOM*, TMT&D Corporation, Mitsubishi Electr. Power Products, Toyo, Japan, Jan. 2017.
[16] *Snapshot of Global Photovoltaic Market 2018*, Int. Energy Agency, Paris, France, Apr. 2018.
[17] *Global Energy Transformation: A Roadmap to 2050*, IRENA Innov. Technol. Center, Bonn, Germany, 2019.
[18] *Technical Guideline: Generating Plants Connected to the Medium-Voltage Network*, BDEW, Berlin, Germany, Jun. 2008.
[19] *Network Code for requirements for Grid Connection Applicable to all Generators*, ENTSOE, Brussels, Belgium, Mar. 2013.
[20] *IEEE Standard for Interconnection and Interoperability of Distributed Energy Resources With Associated Electric Power Systems Interfaces*, IEEE Standard 1547-2018 (Revision of IEEE Std 1547-2003).
[21] *Rule 21: Generating Facility Interconnections*, California, USA, 2018.
[22] *Common Functions for Smart Inverters: 4th Edition*, EPRI, Palo Alto, CA, USA, Dec. 2016.
[23] NREL/SCE, "High-penetration PV integration project: Report on field demonstration of advanced inverter functionality in Fontana, CA," Nat. Renew. Energy Lab., Golden, CO, USA, Tech. Rep. NREL/TP-5D00-62483, Aug. 2014.
[24] B. Mather and A. Gebeyehu, "Field demonstration of using advanced PV inverter functionality to mitigate the impacts of high-penetration PV grid integration on the distribution system," in *Proc. IEEE 42nd Photovoltaic Spec. Conf. (PVSC)*, Jun. 2015, pp. 1–6.
[25] F. Bell, A. Nguyen, M. McCarty, K. Atef, and T. Bialek, "Secondary voltage and reactive power support via smart inverters on a high-penetration distributed photovoltaic circuit," in *Proc. IEEE Power Energy Soc. Innov. Smart Grid Technol. Conf. (ISGT)*, Minneapolis, MN, USA, Sep. 2016, pp. 1–6.
[26] V. Gevorgian and B. O'Neill, "Advanced grid-friendly controls demonstration project for utility-scale PV power plants," Nat. Renew. Energy Lab., Golden, CO, USA, Tech. Rep. NREL/TP-5D00-65368, 2016.
[27] R. K. Varma, V. Khadkikar, and R. Seethapathy, "Nighttime application of PV solar farm as STATCOM to regulate grid voltage," *IEEE Trans. Energy Convers.*, vol. 24, no. 4, pp. 983–985, Dec. 2009.
[28] R. K. Varma, V. Khadkikar, and S. A. Rahman, "Utilization of distributed generator inverters as STATCOM," PCT/CA Patent 2010/001 419, Sep. 15, 2010.
[29] R. K. Varma, S. A. Rahman, and T. Vanderheide, "New control of PV solar farm as STATCOM (PV-STATCOM) for increasing grid power transmission limits during night and day," *IEEE Trans. Power Del.*, vol. 30, no. 2, pp. 755–763, Apr. 2015.
[30] R. K. Varma, "Multivariable modulator controller for power generation facility," PCT/CA Patent 2014 051 174, Dec. 5, 2014.
[31] R. K. Varma and E. M. Siavashi, "PV-STATCOM: A new smart inverter for voltage control in distribution systems," *IEEE Trans. Sustain. Energy*, vol. 9, no. 4, pp. 1681–1691, Oct. 2018.
[32] (Dec. 13, 2016). *Western Engineering Research Demonstrated in Sarnia*. Accessed: Oct. 13, 2019. [Online]. Available: https://www.theobserver.ca/2016/12/13/western-engineering-research-demonstrated-in-sarnia/wcm/48d61f85-3b6c-7e4c-751f-1d896f277fb4
[33] E. M. Siavashi, "Smart PV inverter control for distribution systems," Ph.D. dissertation, Dept. Elect. Comput. Eng., Univ. Western Ontario, London, ON, Canada, 2015. [Online]. Available: https://ir.lib.uwo.ca/etd/3065/
[34] A. Yazdani and R. Iravani, *Voltage-Sourced Converters in Power Systems: Modeling, Control, and Applications*. Hoboken, NJ, USA: Wiley, 2010.
[35] W. Leonhard, *Control of Electrical Drives*. Berlin, Germany: Springer, 2001.
[36] P. P. Dash and A. Yazdani, "A mathematical model and performance evaluation for a single-stage grid-connected photovoltaic (PV) system," *Int. J. Emerg. Electr. Power Syst.*, vol. 9, no. 6, 2008.
[37] C. Loutan *et al.*, "Demonstration of essential reliability services by a 300-MW solar photovoltaic power plant," Nat. Renew. Energy Lab., Golden, CO, USA, Tech. Rep. NREL/TP-5D00-67799, 2017

RAJIV K. VARMA (M'90–SM'09) received the B.Tech. and Ph.D. degrees in electrical engineering from IIT Kanpur, Kanpur, India, in 1980 and 1988, respectively. He is currently a Professor with The University of Western Ontario (UWO), London, ON, Canada. He was the Hydro One Chair in power systems engineering with UWO, from 2012 to 2015. He was a Faculty Member with the Electrical Engineering Department, IIT Kanpur, from 1989 to 2001. He has coauthored an IEEE Press/Wiley book on Thyristor-Based FACTS Controllers. He has co-delivered several tutorials (IEEE sponsored), courses and workshops on smart inverters, FACTS, SVC, and HVDC in different countries. His research interests include FACTS, power systems stability, and grid integration of photovoltaic solar and wind power systems. He is currently the Vice Chair of the IEEE HVDC and FACTS Subcommittee and has been the Chair of the IEEE Working Group 15.05.17 on HVDC and FACTS Bibliography, since 2004.

EHSAN M. SIAVASHI (M'11) received the B.Sc. degree in electrical engineering from the K. N. Toosi University of Technology, in 2007, the M.Sc. degree in power electronics from the University of Tehran, Tehran, Iran, in 2010, and the Ph.D. degree in power systems engineering from The University of Western Ontario, London, ON, Canada, in 2015. He was a Postdoctoral Fellow with The University of Western Ontario, from 2015 to 2017. He is currently a Power Systems Studies Engineer with Powertech Labs Inc., British Columbia, Canada. His current research interests include FACTS, microgrids, power electronics, photovoltaic solar systems, and power quality.

SIBIN MOHAN received the B.Tech. degree in electrical and electronics engineering from Mahatma Gandhi University, India, in 2011, and the M.Tech. degree in electrical engineering (with a specialization in power electronics and power systems) from IIT Bombay, Mumbai, India, in 2014. He is currently pursuing the Ph.D. degree with The University of Western Ontario, London, Canada. He is currently a Research Associate with Bluewater Power Distribution Corporation, Sarnia, ON, Canada. His research interests include smart inverters, distributed generation, FACTS, power system stability, and power quality. He was a recipient of the Industrial Postgraduate Scholarship from Natural Sciences and Engineering Research Council of Canada (NSERC). He has been the Secretary of the IEEE Working Group on HVDC and FACTS Bibliography, since 2015.

TIM VANDERHEIDE was the Vice President of Client Services for Bluewater Power Distribution Corporation. In this role, he was responsible for market services, energy services, metering, billing, and information technologies. He is currently a Chief Operating Officer for Bluewater Power Renewable Energy Inc., and Electek Power Services Inc. He is also the Vice President of Strategic Planning for Bluewater Power Distribution Corporation. He is responsible for the development and implementation of renewable power generation projects for Bluewater Power Renewable Energy Inc., and the Development of New Product and Service Strategies designed to continuously improve shareholder value for Bluewater Power Distribution Corporation. In his role as a Chief Operating Officer for Electek Power Services Inc., he is responsible for overall operations and company growth.